Research Square

Preprints are preliminary reports that have not undergone peer review.
They should not be considered conclusive, used to inform clinical practice,
or referenced by the media as validated information.

# Magneto-polaritons in a wide parabolic quantum well: symmetry breaking and kinetic energy cancellation

**Erika Dias Cabral**

erika.cabral@uerj.br

Rio de Janeiro State University

**Marco Aurélio Boselli**

Federal University of Uberlândia

**Tiago Dourado**

Brazilian Center for Physics Research

**Ivan da Cunha Lima**

University SENAI-Cimatec

**Article**

**Keywords:**

**Posted Date:** June 16th, 2026

**DOI:** https://doi.org/10.21203/rs.3.rs-9886720/v1

**License:** This work is licensed under a Creative Commons Attribution 4.0 International License.
Read Full License

**Additional Declarations:** No competing interests reported.

# Magneto-polaritons in a wide parabolic quantum well: symmetry breaking and kinetic energy cancellation

**E. Dias Cabral[1,*,+], M. A. Boselli[2,+], T. P. Dourado[3,+], and I. C. da Cunha Lima[4,+]**

[1]University of the State of Rio de Janeiro, Rio de Janeiro 23070-200, Brazil
[2]Federal University of Uberlândia 38400-902, Brazil
[3]Brazilian Center of Physical Research, Rio de Janeiro 22290-180, Brazil
[4]University SENAI - CIMATEC, Salvador 41650-010, Brazil
[*]erika.cabral@uerj.br
[+]these authors contributed equally to this work

## ABSTRACT

Magneto-polaritons emerge as hybrid quasiparticle excitations in an electron gas confined by a parabolic potential and subjected to a strong tilted magnetic field. In this work, we provide a rigorous analytical derivation of the Fock-space decoupling procedure that reveals the emergence of two independent harmonic oscillators. We demonstrate that this decoupling leads to the exact cancellation of the free-particle kinetic energy term along the direction orthogonal to the field-confinement plane, even while the associated momentum remains a strictly conserved quantum number. This exact neutralization yields a massive state degeneracy that scales fundamentally with the universal expression of fluxon injection. Furthermore, we map the trajectory of the Fermi level through the hybridized dispersion branches, uncovering discrete jumps that directly govern the localization and transport properties of the magneto-polariton gas. These results establish a robust framework for non-dissipative collective transport in nanoscale heterostructures.

## 1 Introduction

A wide parabolic quantum well (WPQW) is a semiconductor heterostructure engineered by precisely grading the chemical composition of an alloy, typically $Ga_{1-x}Al_xAs$, along the growth direction. By continuously varying the aluminum fraction $x$, the conduction band edge mismatch can be tailored to form a smooth harmonic potential profile for trapped electrons, characterized by a fundamental confinement frequency $\omega_0$.

When WPQWs were first pioneered in the late 1980s and early 1990s[1,2], the primary goal was to create a thick, quasi-three-dimensional electron gas (Q3DEG) capable of hosting high carrier densities while minimizing the effects of spatial charge segregation. In standard square quantum wells, increasing the carrier density causes severe electrostatic screening and band bending, which pushes the electron wave function toward the walls. A parabolic well, conversely, has the unique property that its shape is mathematically invariant under a uniform background charge distribution.

By engineering the harmonic confining potential within a wide spatial geometry ensures that a substantial number of these equally spaced states remain unperturbed by boundary effects at higher energy levels. Combined with the fact that the parabolic profile persists even at elevated electron densities, these unperturbed harmonic oscillator states as an exceptional model for exploring the electronic gas across a wide range of carrier concentrations. The WPQW permits the investigation of many-body correlation effects[3], and the calculation the correlations in the energy spectrum of electrons in a strong magnetic field[4]. Furthermore, the $Ga_{1-x}Al_xAs$ WPQW serves as an ideal platform for investigating magneto-transport under strong fields due to the experimental feasibility of tuning the confinement frequency $\omega_0$ into perfect resonance with the cyclotron frequency $\omega_c$. Since their successful realization, WPQWs have found a diverse array of advanced applications. For instance, they were widely utilized in studying the Quantum Hall Effect[5,6], interband photoluminescence spectroscopy in perpendicular and in-plane magnetic fields[7], terahertz (THz) optics and optoelectronics[8], serving as the active medium for quantum cascade lasers (QCLs)[9], and ultra-high-frequency photodetectors[10]. Magnetoplasma excitations in parabolic quantum wells have been also treated as a fluid with a hydrodynamic model[11].

Magneto-polaritons in semiconductor quantum wells have been extensively studied as hybrid excitations arising from the coupling between harmonic confinement and cyclotron motion in GaAlAs systems[12–14], artificial cavity[15], transition metal dicalcogenides[16] and Weyl semimetals[17]. The problem shares similarities with the Fock-Darwin levels[18,19].

In a recent work[20], we provided a theoretical analysis of magneto-polaritons in a wide parabolic $Ga_{1-x}Al_xAs$ quantum well under a strong magnetic field tilted with respect to the growth direction, yielding the exact energy spectrum and the degeneracy

factor $p = eB/(h\cos\theta)$ as functions of the tilt angle $\theta$. The formalism also contains two deeper structural features that we now explore. The first is the interpretation of the magneto-polariton as a manifestation of symmetry breaking induced by the tilted field. The coupling between the confining potential and the cyclotron motion breaks the rotational symmetry between the transverse directions ($y$ and $z$). The second structural feature is that the transformation leading to the decoupled oscillators also results in the exact cancellation of the kinetic energy along the $x$-direction. It also keeps the momentum $\hat{p}_x$ as a strictly conserved quantity. The eigenvalue of this momentum operator determines the centers of oscillation in the transformed Fock space.

This paper is organized as follows. Section 2 introduces the model. Section 3 addresses the decoupling of the two oscillators and the cancellation of the kinetic energy term. Section 4 shows how this cancellation yields two uncoupled oscillators whose frequencies describe quasi-particles, the magneto-polaritons, mixing Landau levels of frequency $\omega_c$ and harmonic oscillators of frequency $\omega_0$, with characteristic level repulsion near resonance. Section 5 presents dispersion curves, the behavior of the Fermi level through the density of states as the magnetic field and tilt angle are varied, and the dependence of the electron density on the magnetic field, which is connected to Shubnikov oscillations in the three-dimensional electron gas. Finally, Section 6 discusses the results and outlines possible extensions of this work.

## 2 Model

In this work, we treat a gas of electrons in the conduction band of a semiconductor heterostructure, modeled within the effective mass approximation. These electrons are introduced via remote doping, a technique that spatially separates the charge carriers from their ionized impurities. Scattering by these impurities are neglected in the present approach. By precisely grading the aluminum concentration ($x$) in a $Ga_{1-x}Al_xAs$ alloy, the conduction band offset is engineered to create a wide parabolic quantum well (WPQW). This structural grading generates a harmonic confinement potential for the trapped electron gas, characterized by a fundamental oscillator frequency $\omega_0$. Under these conditions, the electron dynamics are governed by quantum harmonic oscillator states, which provide the basis for the subsequent coupling with external magnetic fields.

To complete our model, we consider a magnetic field $\mathbf{B} = (B_x, 0, B_z)$ tilted by an angle $\theta$ relative to the growth direction of the GaAlAs layers. In the effective mass approximation and utilizing the Landau gauge $\mathbf{A} = y(-B_z, 0, B_x)$, the Hamiltonian is given by:

$$H = \frac{1}{2m}\left[(\hat{p}_x - eB_z\hat{y})^2 + \hat{p}_y^2 + (\hat{p}_z + eB_x\hat{y})^2\right] + \frac{1}{2}m\omega_0^2\hat{z}^2 + g_0\mu_B\mathbf{B}\cdot\boldsymbol{\sigma}. \tag{1}$$

where $\sigma = \pm 1/2$ denotes the spin projection along the field direction. The hats identify operators, while $m$ and $g_0$ are the effective mass for electrons in the conduction band of GaAs, and their respective Landé factor.

The first observations concerning the Hamiltonian in Eq. (1) is that, once the choice for the Landau gauge made with a magnetic field components on the $x$ and $z$ directions, we obtain $[\hat{p}_x, H] = 0$. It means that the eigenstates of the Hamiltonian are also eigenstates of the momentum operator in the $x$-direction. In this case we can substitute $\hat{p}_x$ directly by its eigenvalue $p_x = \hbar k_x$, say. On the other hand, neither $\hat{p}_y$ nor $\hat{p}_z$ commute with the Hamiltonian, and to make the problem complex, the square involving $\hat{p}_z$ and $\hat{y}$ couples the motions in these two directions. As a second observation, the first square in parenthesis seems to introduce a kinetic energy in the $x$ degree of freedom, although not coupling the motion in the $x$ and $y$ directions. As we have shown in a previous publication[20], the cancellation of the kinetic energy reduces the problem to two coupled oscillators giving rise to a quasi-particle called magneto-polariton. The aim of this work is to demonstrate this exat cancellation and discuss the consequences of conserving the momentum without generating a kinetic energy.

The general problem of coupled harmonic oscillators in a magnetic field was solved analytically by Merlin[21], demonstrating that a transformation of coordinates leads to two independent normal modes.

At this point we start using the basis $|x, y, p_z\rangle$, eigenstates of the non-commuting operators $\hat{x}$, $\hat{y}$, $\hat{p}_z$:

$$\begin{aligned}
\hat{x}|x,y,p_z\rangle &= x|x,y,p_z\rangle \\
\hat{y}|x,y,p_z\rangle &= y|x,y,p_z\rangle \\
\hat{z}|x,y,p_z\rangle &= i\hbar\tfrac{\partial}{\partial p_z}|x,y,p_z\rangle \\
\hat{p}_x|x,y,p_z\rangle &= -i\hbar\tfrac{\partial}{\partial x}|x,y,p_z\rangle \\
\hat{p}_y|x,y,p_z\rangle &= -i\hbar\tfrac{\partial}{\partial y}|y,p_z\rangle \\
\hat{p}_z|x,y,p_z\rangle &= p_z|x,y,p_z\rangle
\end{aligned} \tag{2}$$

In this representation, the Hamiltonian takes the form:

$$H = \frac{p_x^2}{2m}\sin^2\theta + \frac{\hat{p}_y^2}{2m} + \frac{1}{2}m\omega_c^2(y-y_0)^2 + \frac{p_z^2}{2m} - \frac{\hbar^2 m\omega_0^2}{2}\frac{\partial^2}{\partial p_z^2} + \omega_c \sin\theta\ y p_z + g_0\mu_B \mathbf{B}\cdot\sigma \tag{3}$$

## 3 Decoupling the oscillators

For the sake of making it easier to follow the demonstration of the appearance of the magneto-polaritons, we introduce here details of the decoupling after a rotation in the Fock space, the cancellation of the kinetic term in one direction, and the preservation of the momentum in that direction as a conserved quantity, details not presented in our previous publication[20].

The term before last in Eq. (3), couples a harmonic oscillator in the $p_z$ variable with a harmonic oscillator in the $y$ variable. It is preferable to change the notation to obtain the coupling between variables of dimension length,

$$\begin{aligned} p_z &= a\eta \\ z &= i\hbar\tfrac{\partial}{a\partial\eta} \end{aligned} \tag{4}$$

and finding $a$ so that we obtain the standard expression of the harmonic oscillator in $\eta$. For this, we set:

$$\frac{\hbar^2 m\omega_0^2}{2}\frac{\partial^2}{\partial p_z^2} = \frac{\hbar^2}{2m}\frac{\partial^2}{\partial\eta^2} \tag{5}$$

and we obtain $a = m\omega_0$, consequently:

$$\eta = \frac{p_z}{m\omega_0}. \tag{6}$$

Notice that $\eta$ is not a position variable in real space, but the momentum in the z-direction scaled by a parameter depending on $\omega_0$. Substituting the change of basis into the Hamiltonian with

$$\frac{p_z^2}{2m} = \frac{a^2\eta^2}{2m} = \frac{1}{2}m\omega_0^2\eta^2 \tag{7}$$

we obtain:

$$H = \frac{p_x^2}{2m}\sin^2\theta + \frac{p_y^2}{2m} + \frac{1}{2}m\omega_c^2(y-y_0)^2 + \frac{p_\eta^2}{2m} + \frac{1}{2}m\omega_0^2\eta^2 + m\omega_c\omega_0\sin\theta\ y\eta + g_0\mu_B\mathbf{B}\cdot\sigma, \tag{8}$$

with

$$y_0 = \frac{p_x cos\theta}{m\omega_c} \tag{9}$$

We now observe that the Hamiltonian consists of four contributions. The first is a free (anomalous) motion in the $x$ direction of a particle with effective mass $m_{\text{eff}} = m/\sin^2\theta$. The second is a quantum oscillator of a particle of mass $m$ in the $y$ direction, with oscillation frequency $\omega_c$, centered at $y = y_0$, which is a real position coordinate. The third is a degree of freedom corresponding to a quantum oscillator of a particle of mass $m$ in the $\eta$ direction, not a real position coordinate, but an entry which is a vector basis in the Fock space, with frequency $\omega_c$, centered at $\eta = 0$, corresponding to $p_z = 0$. The fourth is a coupling between the two oscillators. It is of great importance to draw attention to the apparent kinetic energy term, which appears multiplied by a $\sin^2\theta$. We will return to this point later on. Let us write the terms to be treated separately in Eq. (8) as:

$$T = \frac{1}{2}m\omega_c^2(y-y_0)^2 + \frac{1}{2}m\omega_0^2\eta^2 + m\omega_c\omega_0\sin\theta\ y\eta \tag{10}$$

To proceed with the decoupling, we perform a rotation of the axes counter-clockwise by an angle $\alpha$. The kinetic energy terms do not change, since it is expressed by the scalar product of the momentum operator with itself. The relationship between the old coordinates $\eta$ and $y$ with the new coordinates $\eta'$ and $y'$ that represent the decoupled oscillators is:

$$\begin{pmatrix} y \\ \eta \end{pmatrix} = \begin{pmatrix} \cos\alpha & -\sin\alpha \\ \sin\alpha & \cos\alpha \end{pmatrix} \begin{pmatrix} y' \\ \eta' \end{pmatrix} = \begin{pmatrix} a & b \\ -b & a \end{pmatrix} \begin{pmatrix} y' \\ \eta' \end{pmatrix} \tag{11}$$

The required rotation for decoupling is given by the solution of

$$\omega_c \omega_0 \sin\theta \cos 2\alpha = \frac{1}{2}(\omega_c^2 - \omega_0^2) \sin 2\alpha. \tag{12}$$

With this:

$$\tan 2\alpha = 2\frac{\omega_c \omega_0}{\omega_c^2 - \omega_0^2} \sin\theta. \tag{13}$$

This rotation allows the term in Eq. (10) to be written as quadratic forms, making $T$ to be expressed like harmonic potentials:

$$T = A(y' - y'_0)^2 + B(\eta' - \eta'_0)^2 + C, \tag{14}$$

We are left to identify the coefficients $A$, $B$, and the independent term $C$. In the rotated frame we have:

$$\begin{aligned} T = & \quad [\frac{1}{2}m\omega_c^2 a^2 + \frac{1}{2}m\omega_0^2 b^2 - m\omega_c\omega_0 \sin\theta ab]y'^2 \\ & + \quad [-m\omega_c^2 a y_0]y' + \frac{1}{2}m\omega_c^2 y_0^2 \\ & + \quad [\frac{1}{2}m\omega_c^2 b^2 + \frac{1}{2}m\omega_0^2 a^2 + m\omega_c\omega_0 \sin\theta ab]\eta'^2 \\ & + \quad [-m\omega_c^2 b y_0]\eta' \end{aligned} \tag{15}$$

Defining:

$$\begin{aligned} A_x &= \frac{1}{2}m\omega_c^2 y_0^2 = \frac{p_x^2}{2m}\cos^2\theta \\ A_1 &= \frac{1}{2}m\omega_c^2 a^2 + \frac{1}{2}m\omega_0^2 b^2 - m\omega_c\omega_0 \sin\theta ab \\ A_2 &= -m\omega_c^2 a y_0, \end{aligned} \tag{16}$$

and

$$\begin{aligned} B_1 &= \frac{1}{2}m\omega_c^2 b^2 + \frac{1}{2}m\omega_0^2 a^2 + m\omega_c\omega_0 \sin\theta ab \\ B_2 &= -m\omega_c^2 b y_0. \end{aligned} \tag{17}$$

Eq. (15) can now be written as:

$$\begin{aligned} T &= A_1 y'^2 + A_2 y' + B_1 \eta'^2 + B_2 \eta' + A_x \\ &= A_1\left(y' + \frac{A_2}{2A_1}\right)^2 + B_1\left(\eta' + \frac{B_2}{2B_1}\right)^2 - \frac{A_2^2}{4A_1} - \frac{B_2^2}{4B_1} + A_x. \end{aligned} \tag{18}$$

The last three terms in Eq. (18) are identifyed as the independent term $C$ in Eq. (14):

$$C = -\frac{A_2^2}{4A_1} - \frac{B_2^2}{4B_1} + A_x = -\frac{B_1 A_2^2 + A_1 B_2^2}{4A_1 B_1} + A_x \tag{19}$$

The numerator in equation (19) becomes:

$$B_1A_2^2+A_1B_2^2=\frac{1}{2}m^3\omega_c^4y_0^2\omega_0^2. \tag{20}$$

At this point it is important to call attention to the appearance of $y_0$ in the decoupling. Recall that Eq. (9) it is determined by $p_x$, which now enters in the decoupling process. For the denominator of Eq. (19), we have:

$$4A_1B_1=m^2\omega_c^2\omega_0^2\cos^2\theta. \tag{21}$$

Finally, the complicated fraction in equation (19) reduces to the negative expression of a kinetic energy in the $x$-direction, after using the definition of $y_0$ in Eq. (9):

$$-\frac{B_1A_2^2+A_1B_2^2}{4A_1B_1}=-\frac{\frac{1}{2}m^3\omega_c^4y_0^2\omega_0^2}{m^2\omega_c^2\omega_0^2\cos^2\theta}=-\frac{\frac{1}{2}m\omega_c^2y_0^2}{\cos^2\theta}=-\frac{p_x^2}{2m}. \tag{22}$$

Therefore the contribution of independent term to the Hamiltonian becomes:

$$C=-\frac{p_x^2}{2m}+\frac{p_x^2}{2m}\cos^2\theta=-\frac{p_x^2}{2m}\sin^2\theta. \tag{23}$$

As we intended to demonstrate, this term cancels identically the anomalous kinetic energy in the $x$-direction of the Hamiltonian in Eq. (8), $p_x^2\sin^2\theta/2m$, while keeping the states as eigenstates of the momentum in the $x$-direction, leading to the degeneracy of the eigenstates of the Hamiltonian of the system of non-interacting electrons:

$$\begin{aligned} H &= \frac{p_y^2}{2m}+\frac{1}{2}m\omega_c^2(y-y_0)^2+\frac{p_\eta^2}{2m}+\frac{1}{2}m\omega_0^2\eta^2 \\ &+ m\omega_c\omega_0\sin\theta\ y\eta+g_0\mu_B\mathbf{B}\cdot\sigma, \end{aligned} \tag{24}$$

Notice that we cannot consider the degeneracy of this Hamiltonian as that of the two-dimensional Landau levels by just substituting the magnetic field by its z-component, $B\cos\theta$. The symmetry breaking makes these states to be localized as harmonic oscillators in a two-dimensional Fock space of coordinates $y'$ and $\eta'$.

## 4 The magneto-polariton

We now define the frequencies $\Omega_a,\Omega_b$ and the centers $y_0',\eta_0'$ and the energy constant of the two decoupled oscillators:

$$\begin{aligned} A_1 &\doteq \frac{1}{2}m\Omega_a^2,\quad y_0'=-\frac{A_2}{2A_1}=\frac{\omega_c^2}{\Omega_a^2}\cos\alpha y_0 \\ B_1 &\doteq \frac{1}{2}m\Omega_b^2,\quad \eta_0'=-\frac{B_2}{2B_1}=-\frac{\omega_c^2}{\Omega_b^2}\sin\alpha y_0 \end{aligned} \tag{25}$$

Therefore, with the help of Eqs. (16 ) and (17), we obtain the frequencies of the oscillators and their centers of oscillation:

$$\Omega_a=\sqrt{\omega_c^2\cos^2\alpha+\omega_0^2\sin^2\alpha+\omega_c\omega_0\sin\theta\sin2\alpha},\quad y_0'=y_0\frac{\omega_c^2}{\Omega_a^2}\cos\alpha; \tag{26}$$

$$\Omega_b=\sqrt{\omega_c^2\sin^2\alpha+\omega_0^2\cos^2\alpha-\omega_c\omega_0\sin\theta\sin2\alpha},\quad \eta_0'=-y_0\frac{\omega_c^2}{\Omega_b^2}\sin\alpha; \tag{27}$$

To conclude with the decoupling, the Hamiltonian for the electron gas becomes:

$$H=\left[\frac{p_{y'}^2}{2m}+\Omega_a^2(y'-y_0')^2\right]+\left[\frac{p_{\eta'}^2}{2m}+\Omega_b^2(\eta'-\eta_0')^2\right]+g_0\mu_B\mathbf{B}\cdot\sigma, \tag{28}$$

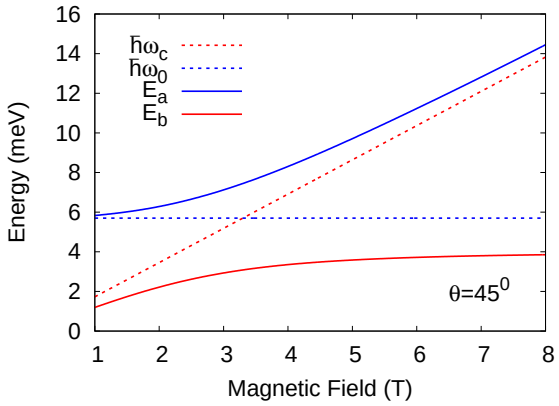



**Figure 1.** The magneto-polariton showing a typical polariton dispersion relation.The two branches coincide with the cyclotron frequency and the natural frequency of the confining parabolic potential at small magnetic field, and exchange their nature at strong magnetic field. After Ref.[20].

with the Schrödinger equation

$$H|n_a,n_b,k_x,\sigma\rangle = E_{n_a,n_b,k_x,\sigma}|n_a,n_b,k_x,\sigma\rangle, \tag{29}$$

with

$$E_{n_a,n_b,k_x,\sigma} = E_a(n_a+1/2)+E_b(n_b+1/2)+g_0\mu_B\mathbf{B}\cdot\sigma. \tag{30}$$

The indexes $n_a, n_b$ label the occupation numbers for an oscillators type $a$ centered at $y_0'$, and another type $b$ centered in $\eta_0'$. Although the Hamiltonian does not contain a term in the x-direction, its eigenstates are also eigenstates of the operator $\hat{p}_x$:

$$\hat{p}_x|n_a,n_b,k_x,\sigma\rangle = \hbar k_x|n_a,n_b,k_x,\sigma\rangle, \tag{31}$$

In consequence,

$$\Psi_{n_a,n_b,k_x\sigma}(x,y',\eta',\sigma) = \frac{1}{\sqrt{L_x}}\exp(ik_x x)\psi_{n_a}(y'-y_0')\psi_{n_b}(\eta'-\eta_0')\Phi(\sigma), \tag{32}$$

where $\psi_n(y-y_0)$ represents the harmonic oscillator wavefunction. The value of $k_x$ determines the centers of the oscillations *via* $y_0$:

$$y_0 = \frac{\hbar k_x}{m\omega_c}\cos\theta \tag{33}$$

Figure 1 shows the dispersion relation for the magneto polariton for a tilt angle of $45^0$ in the interval for the magnetic field from 1-8 T. We observe the typical polariton repulsion of the curves near resonance. The decoupling of the Hamiltonian provides a linear dependence of the gap in the dispersion curves of the magneto-polariton at resonance, $\omega_c = \omega_0$. As established in the derivation of the normal modes, the relationship between the decoupling angle $\alpha$ and the system parameters is governed by:

$$\omega_c\omega_0\sin\theta\cos 2\alpha = \frac{1}{2}(\omega_c^2-\omega_0^2)\sin 2\alpha. \tag{34}$$

At the resonance condition, where the cyclotron frequency matches the structural confinement frequency ($\omega_c = \omega_0$), the right-hand side of Eq. (34) vanishes. Consequently, the relation simplifies to:

$$\omega_c\omega_0\sin\theta\cos 2\alpha = 0. \tag{35}$$

This condition holds for any non-zero tilt angle $\theta$, implying that at resonance, the decoupling angle is fixed at $\alpha = \pi/4$. Substituting this value into the expressions for the normal mode frequencies $\Omega_a$ and $\Omega_b$, we define the gap between the dispersion branches at resonance as $\Delta_g = \Omega_a - \Omega_b$:

$$\Delta_g = \omega_0\left[\sqrt{1+\sin\theta}-\sqrt{1-\sin\theta}\right]. \tag{36}$$

A Taylor expansion of the terms within the brackets reveals that for a wide range of tilt angles, the expression $\sqrt{1+\sin\theta} - \sqrt{1-\sin\theta}$ approximates to $\theta$ with remarkable precision. Thus, at the resonance point, the gap follows a simple linear scaling:

$$\Delta_g = \omega_0 \theta. \tag{37}$$

Figure 2 illustrates the linear dependence of the energy gap at resonance ($\omega_c/\omega_0 = 1$), and those of two detuned cases, $\omega_c/\omega_0 = 0.8$ and 1.2. We observe that beyond a critical tilt angle, the curve corresponding to the higher magnetic field ($\omega_c/\omega_0 \geq 1$) deviates and intersects the linear resonance line.

In terms of the eigenenergies given by Eq. (30), the energy gap $E_g = E_a - E_b$ for a given magnetic field and tilt angle corresponds to the energy necessary to make a transition from a state $|n_a, n_b, k_x, \sigma\rangle$ to a state $|n'_a, n'_b, k_x, \sigma\rangle$ with the selection rules $n'_a = n_a + 1$, $n'_b = n_b - 1$.

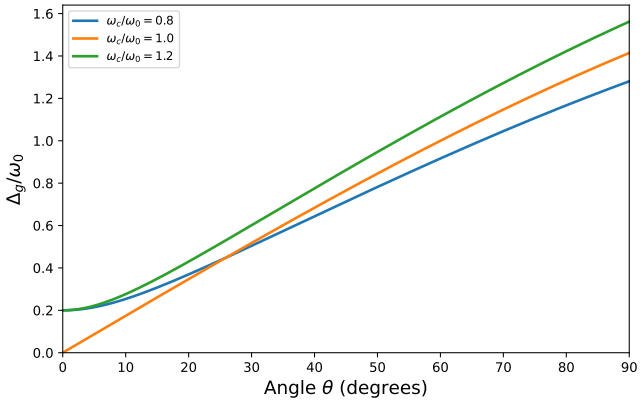



**Figure 2.** Linear dependence of the energy gap at resonance ($\omega_c/\omega_0 = 1$), and those of two detuned cases, $\omega_c/\omega_0 = 0.8$ and 1.2.

## 5 Energy dispersion curves and the Fermi level

Figure 3 illustrates the electron energy dispersion relations of Eq. (30) for a magnetic field range of 1–8 T at a tilt angle of $\theta = 45°$. Note that spin splitting is not clearly resolved at this energy scale. The quantum numbers $(n_a, n_b)$ identify each branch are indicated in parentheses. The eigenstates of the system Hamiltonian are degenerate due to the absence of kinetic energy in $x$ as we showed in[20], the degeneracy being:

$$p = \frac{B}{\cos\theta} \times \frac{e}{h}. \tag{38}$$

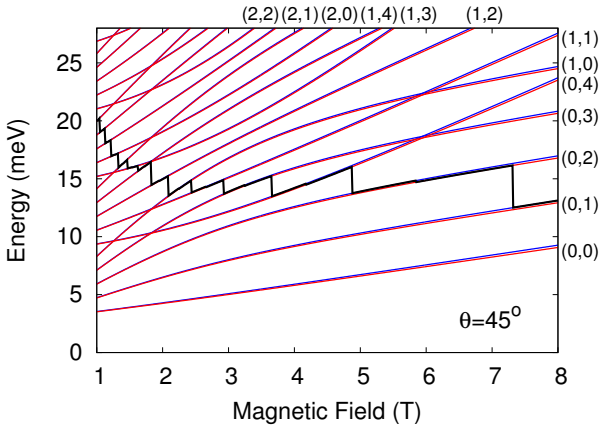



**Figure 3.** Dispersion relations $E_a(n_a+1) + E_b(n_b+1)$ for $B$ in the range 1-8 T, and $\theta = 45^o$. After Ref.[20].

It is worth noting that while some branches are allowed to cross, others exhibit repulsion (anti-crossing), appearing as pairs of branches with opposing curvatures. This behavior follows a specific selection rule: energy dispersion curves $E(n_a, n_b; k_x; \sigma)$ belonging to a family $n_a$ never crosses each other. Near $B_0 = m\omega_0/e$, if $n_b < n_a$ all the energy dispersion curves bend up, the larger the difference between indexes, the larger the curvature; if $n_b > n_a$ all the energy dispersion curves bend down, and the larger the difference, the larger the curvature, again. The same behavior is observed for curves belonging to the family $n_b$. However, curves $E(n_a, n_b; k_x; \sigma)$ may cross with higher-lying curves $E(n'_a, n'_b; k_x; \sigma)$ if $n_a > n_b$ and $n'_a < n'_b$.

The degeneracy is equal for all states $|n_a, n_b, k_x, \sigma\rangle$. The filling factor $q$ is given by:

$$q = \frac{p}{n_s}, \tag{39}$$

for a surface electron density $n_s$. The trajectory followed by the Fermi level as the magnetic field increases consists of a sequence of segments tracking the dispersion curve of a specific branch. During these phases, the branch is gradually depopulated as the increasing degeneracy $p$ redistributes electrons into lower-lying states. When a branch is completely emptied, the Fermi level undergoes a discrete vertical jump to the branch immediately below. Figure 3 indicates that at $B = 5$ T, the Fermi level resides on the $(0,2)$ branch.

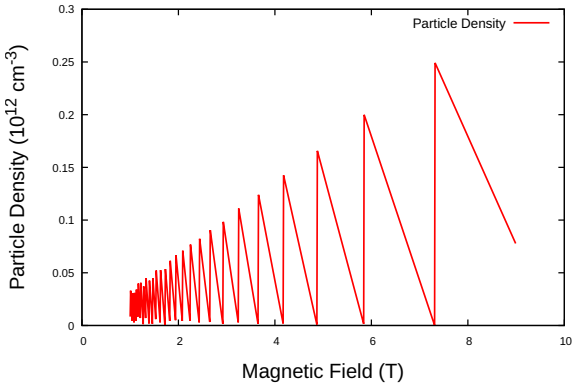



**Figure 4.** Density of electrons at the Fermi level showing the Shubnikov-de Hass oscillations.

Once the Fermi level is determined as a function of the magnetic field for a fixed tilt angle, we can calculate the electron density at the Fermi level:

$$\rho(E_F) = n_s \left(1 - n_{occ} \frac{p}{n_s}\right), \tag{40}$$

where $n_s$ is the two-dimensional electron density (number of electrons per unit area in the $x$-$y$ plane) and $n_{occ}$ is the number of fully occupied branches below the Fermi level. Figure 4 displays the resulting Shubnikov-de Haas like oscillations. This calculation does not account for disorder (e.g., from impurity scattering), which results in the observed sharp peaks and linear jumps. The slope of the linear segments to the right of the peaks—representing the path of the Fermi level along a fixed branch—decreases as the degeneracy $p$ grows linearly with the magnetic field.

Observing the path of the Fermi level in Fig. 3, we see that, as the magnetic field strength increases, the hoping occurs decreasing $n_b$ by steps of two, up to $n_b = 0$, for $n_b$ even, or $n_b = 1$, for $n_b$ odd. Next it jumps no the next branch with $n_a - 1$. In terms of localization, this means that as the magnetic field increases, the magneto-polariton starts being more localized in the $\eta'$ dimension before starting the increasing of its localization in the $y'$ dimension. These changes in the localization are, however, discontinuous.

## 6 Concluding Remarks

In conclusion, the microscopic physics of magneto-polaritons in a wide parabolic quantum well under a tilted magnetic field reveals an interplay between symmetry breaking, quantum conservation laws, and localized transport. The essence of this work lies in how the system resolves the coupling introduced by the tilted configuration of the external magnetic field relative to the parabolic confinement axis. While a standard perpendicular field can be treated using a symmetric Landau gauge, the broken symmetry of the tilted field necessitates an asymmetric gauge configuration, coupling the spatial degrees of freedom.

The coupling is completely resolved by a unitary rotation within the two-dimensional Fock space. The immediate consequence of this decoupling transformation is the exact, analytical cancellation of the free-particle kinetic energy term along the direction perpendicular to the plane formed by the magnetic field and the confinement axis. Despite the complete neutralization of the kinetic energy in this specific direction, the corresponding momentum operator commutes with the decoupled Hamiltonian and remains a conserved quantum number.

The suppression of kinetic energy alongside the conservation of momentum constitutes the mechanism governing the electron gas. Rather than propagating freely, this conservation forces the electronic states to localize as quantum harmonic oscillators, centered at coordinates within the Fock dimensions that are determined by the conserved momentum itself. Furthermore, this restriction yields a macroscopic state degeneracy that satisfies the universal rules associated with the injection of magnetic fluxons into the heterostructure.

## Acknowledgement

We acknowledge the financial support of the PCI/MCTI/CNPQ Grant No. 300409/2026-5 and the financial support of FAPERJ Grant No. E26/010.002385/2019, also acknowledge the financial support of the FAPEMIG Grant No. APQ-00924-23 and Grant No. MCTI/CNPq/CAPES/FAPS16/2014.

## Author contributions statement

All authors contributed equally. All authors reviewed the manuscript.

## Additional information

**Competing interests** The authors declare no competing interests.

## References

1. Mitsuo Kawabe, Masahumi Kondo, Nobuyuki Matsuura, and Kenya Yamamoto. Photoluminescence of $Al_xGa_{1-x}As/Al_yGa_{1-y}As$ multiguantum wells grown by pulsed molecular beam epitaxy. *Japanese Journal of Applied Physics*, **22**(2A), L64. DOI 10.1143/JJAP.22.L64 (1983).

2. R. C. Miller, A. C. Gossard, D. A. Kleinman, and O. Munteanu. Parabolic quantum wells with the GaAs–$Al_xGa_{1-x}As$ system. *Phys. Rev. B*, **29**:3740(R)–3743(R), DOI 10.1103/PhysRevB.29.3740 (1984).

3. I. K. Marmorkos and S. Das Sarma. Interacting intersubband excitations in parabolic semiconductor quantum wells. *Phys. Rev. B*, **48**, 1544–1561, DOI 10.1103/PhysRevB.48.1544 (1993).

4. Luis Brey. Energy spectrum of electrons in a parabolic quantum well in a strong magnetic field. *Phys. Rev. B*, **44**, 3772–3781, DOI 10.1103/PhysRevB.44.3772 (1991).

5. E. G. Gwinn, R. M. Westervelt, P. F. Hopkins, A. J. Rimberg, M. Sundaram, and A. C. Gossard. Quantum Hall effect in wide parabolic GaAs/$Al_xGa_{1-x}As$ wells. *Phys. Rev. B*, **39**, 6260(R)–6263(R), DOI 10.1103/PhysRevB.39.6260 (1989).

6. C. E. Hembree, B. A. Mason, A. Zhang, and J. A. Slinkman. Subband spectrum of a parabolic quantum well in a perpendicular magnetic field. *Phys. Rev. B*, **46**, 7588–7592, DOI 10.1103/PhysRevB.46.7588 (1992).

7. T. Sajoto, J. Jo, M. Santos, and M. Shayegan. High quality electron system with variable electron layer thickness in a parabolic quantum well. *Applied Physics Letters*, **55**, 1430–1432, DOI https://doi.org/10.1016/0039-6028(90)90840-5 (1989).

8. R. Bratschitsch, T. Müller, R. Kersting, G. Strasser, and K. Unterrainer. Coherent terahertz emission from optically pumped intersubband plasmons in parabolic quantum wells. *Applied Physics Letters*, **76**, 3501–3503, DOI 10.1063/1.126687 (2000).

9. Claire Gmachl, Federico Capasso, Deborah L Sivco, and Alfred Y Cho. Recent progress in quantum cascade lasers and applications. *Reports on Progress in Physics*, **64**, 1533, DOI 10.1088/0034-4885/64/11/204 (2001).

10. P.D. Grant, R. Dudek, M. Buchanan, L. Wolfson, and H.C. Liu. An ultra fast quantum well infrared photodetector. *Infrared Physics & Technology*, **47**, 144–152, DOI https://doi.org/10.1016/j.infrared.2005.02.019 (2005).

11. Jed Dempsey and B. I. Halperin. Magnetoplasma excitations in parabolic quantum wells: Hydrodynamic model. *Phys. Rev. B*, **45**, 1719–1735, DOI 10.1103/PhysRevB.45.1719 (1992).

**12.** G. M. Gusev, A. A. Quivy, T. E. Lamas, J. R. Leite, A. K. Bakarov, A. I. Toropov, O. Estibals, and J. C. Portal. Magnetotransport of a quasi-three-dimensional electron gas in the lowest Landau level. *Phys. Rev. B*, **65**, 205316, DOI 10.1103/PhysRevB.65.205316 (2002).

**13.** C. A. Duarte, G. M. Gusev, A. A. Quivy, T. E. Lamas, A. K. Bakarov, and J. C. Portal. Landau-level crossing in two-subband systems in a tilted magnetic field. *Phys. Rev. B*, **76**, 075346, DOI 10.1103/PhysRevB.76.075346 (2007).

**14.** H. W. Jiang and Eli Yablonovitch. Gate-controlled electron spin resonance in GaAs/$Al_xGa_{1-x}As$ heterostructures. *Phys. Rev. B*, **64** 041307(R). DOI 10.1103/PhysRevB.64.041307 (2001).

**15.** G. Scalari, C. Maissen, D. Turčinková, D. Hagenmüller, S. De Liberato, C. Ciuti, C. Reichl, D. Schuh, W. Wegscheider, M. Beck, and J. Faist. Ultrastrong coupling of the cyclotron transition of a 2D electron gas to a Thz metamaterial. *Science*, **335**, 1323–1326. DOI 10.1126/science.1216022 (2012).

**16.** Bo Han, Jamie M. Fitzgerald, Lukas Lackner, Roberto Rosati, Martin Esmann, Falk Eilenberger, Takashi Taniguchi, Kenji Watanabe, Marcin Syperek, Ermin Malic, and Christian Schneider. Infrared magnetopolaritons in $MoTe_2$ monolayers and bilayers. *Phys. Rev. Lett.*, **134**, 076902. DOI 10.1103/PhysRevLett.134.076902 (2025).

**17.** Zhongqu Long, Yongrui Wang, Maria Erukhimova, Mikhail Tokman, and Alexey Belyanin. Magnetopolaritons in Weyl semimetals in a strong magnetic field. *Phys. Rev. Lett.*, **120**, 037403. DOI 10.1103/PhysRevLett.120.037403 (2018).

**18.** V. Fock. Bemerkung zur Quantelung des harmonischen Oszillators im Magnetfeld. *Zeitschrift für Physik*, **47**, 446–448. DOI 10.1017/S0305004100015655 (1928).

**19.** C. G. Darwin. The diamagnetism of free electrons. *Proceedings of the Cambridge Philosophical Society*, **27**, 86–90. DOI 10.1017/S0305004100015655 (1930).

**20.** T. P. Dourado, E. Dias Cabral, M. A. Boselli, and I. C. da Cunha Lima. Magneto-polariton: Strong tilted magnetic field applied on confined electron gas in a wide $Ga_{1-x}Al_xAs$ quantum well. *Journal of Applied Physics*, **135**, 115704. DOI 10.1063/5.0190812 (2024).

**21.** R. Merlin. Coupled harmonic oscillators in a magnetic field. *Solid State Communications*, **64**, 99–101. DOI 10.1016/0038-1098(87)90929-7 (1987).